Chemical Physics Letters 803 (2022) 139800

Contents lists available at ScienceDirect

Chemical Physics Letters

journal homepage: www.elsevier.com/locate/cplett

Spectroscopy of *N*-methylpyrrole-RG (RG = Ar, Kr) complexes: First excited neutral and ground cationic states

Alexander R. Davies, Jessica T.L. Haynes, Timothy G. Wright

School of Chemistry, University of Nottingham, University Park, Nottingham NG7 2RD, UK

ARTICLE INFO

Keywords:
N-methylpyrrole
Rare gas
Complexes
REMPI
ZEKE
Ionization

ABSTRACT

N-methylpyrrole-RG (RG = Ar, Kr) complexes are investigated using resonance-enhanced multiphoton ionization (REMPI) and zero-electron-kinetic-energy (ZEKE) spectroscopy. The RG atom makes the electronic transition to the S_1 state allowed, and the REMPI spectrum is blue-shifted compared to the *N*-methylpyrrole origin, with no bands associated with vibrational excitation of the *N*-methylpyrrole moiety. The nature of the electronic structure of the S_1 state is discussed. Binding energies are obtained for all three electronic states. Adiabatic ionization energies are obtained from the ZEKE spectra, yielding values of $64077 \pm 5\ cm^{-1}$ and $64029 \pm 5\ cm^{-1}$ for RG = Ar and Kr, respectively.

1. Introduction

In recent work [1-4], we have examined the electronic spectroscopy of the S_1 electronic state of *N*-methylpyrrole (NMP), probing the vibronic interactions using two-dimensional laser-induced fluorescence (2D-LIF), resonance-enhanced multiphoton ionization (REMPI), and zero-electron-kinetic-energy (ZEKE) spectroscopy. The work built upon earlier spectroscopic [5-9] and photodissociation [10-16] studies by a number of workers; additionally, very recently a far infrared spectrum of NMP has been reported [17]. The S_1 state of NMP is found to be a largely Rydberg-like 3s state in the Franck-Condon region of the S_1 ($^1A_2$) ← S_0 ($^1A_1$) transition, but at extended N–CH_3 bond lengths, the state evolves into a σ* state. Although there has been a microwave study [18] of NMP–Ar, which concluded the Ar atom is located above the pyrrolyl ring in the ground electronic state, we are unaware of any studies on excited or cationic states of complexes of NMP, which we rectify herein by reporting REMPI and ZEKE spectra of NMP–RG (RG = Ar, Kr). Part of the impetus for this is to investigate whether the perturbation of the electronic structure by the RG atom is sufficient to render the origin transition symmetry allowed, as well as to see whether it is possible to observe intermolecular and torsional motion for such complexes. The ZEKE spectra would also be expected to yield ionization energies and, together with the REMPI spectra, binding energies in the different states should be available. This would be the first step in investigating the role of solvation on this forbidden electronic transition. This also opens up the possibility of undertaking ultrafast experiments to see how solvation affects the photophysics of NMP and perhaps pyrrole itself – a key chromophore in many biomolecules.

2. Experimental

The REMPI/ZEKE [19] apparatus is the same as that employed in our recent studies on NMP [1-3]. In all of the present experiments, a free-jet expansion of the vapour above room-temperature NMP liquid (Sigma-Aldrich, 99% purity) was employed. For the NMP–Ar complexes, the backing gas was pure Ar at a pressure of 3 bar, while for the NMP–Kr complexes, mixtures of 20–40% Kr in Ar were employed, with a total pressure of 2–3 bar.

For the one-colour REMPI experiments, we employed the frequency-doubled output of a dye laser (Sirah CobraStretch), operating with Coumarin 480 and pumped with the third harmonic of a Surelite III Nd:YAG laser. For the two-colour REMPI and ZEKE spectra of NMP, the focused outputs of two dye lasers (Sirah CobraStretch) were overlapped spatially and temporally, and passed through a vacuum chamber coaxially and counterpropagating, where they intersected the free-jet expansion. The excitation laser was the same for all REMPI and ZEKE experiments, while the ionization laser for the two-colour REMPI and ZEKE experiments operated with Coumarin 440, pumped with the third harmonic (355 nm) of a Surelite I Nd:YAG laser, and the fundamental output was employed.

The jet expansion passed between two biased electrical grids located in the extraction region of a time-of-flight mass spectrometer, which was employed in the REMPI experiments. These grids were also used in the ZEKE experiments by application of pulsed voltages, giving typical fields

E-mail address: Tim.Wright@nottingham.ac.uk (T.G. Wright).

https://doi.org/10.1016/j.cplett.2022.139800
Received 30 March 2022; Received in revised form 13 June 2022; Accepted 15 June 2022
Available online 19 June 2022

of ~10 V cm^{-1}, after a delay of ~2 μs (this delay was minimized while avoiding the introduction of excess noise from the prompt electron signal). The resulting ZEKE bands had widths of ~5–7 cm^{-1}. The electron and ion signals were each recorded on a separate set of microchannel plates.

3. Quantum chemistry

Quantum chemistry calculations were undertaken using density functional theory, for which we employed the CAM-B3LYP functional [20] to better-describe long-range interactions than the B3LYP functional itself, which we had used previously for NMP [2,3].

We optimized the geometries of three different isomers of the S_0 and D_0^+ states using the (U)CAM-B3LYP/aug-cc-pVTZ level of theory: one with the RG atom above the NMP ring, one with the RG approaching the methyl group, and one with the RG approaching the NMP molecule from the opposite end from the methyl group – see Figure S1 of the Supplementary Material. These calculations indicated that the lowest-energy isomer was the one with the RG atom above the ring, in agreement with the results of a microwave study [18].

We also calculated binding energies for the S_0 and D_0^+ states. This was done at the CAM-B3LYP level by simply subtracting the energy of the complex from that of each of the RG and NMP species, with the latter at its (U)CAM-B3LYP/aug-cc-pVTZ-optimized geometry. Single-point (R)CCSD(T) calculations using the same geometry and basis set were also undertaken, and counterpoise-corrections were undertaken to obtain the basis set superposition error (BSSE). This was obtained for each moiety at the complex geometry and was then subtracted from the aforementioned calculated binding energy. The latter calculations confirmed that the lowest-energy isomer was the ring-bound one, again consistent with the results of a microwave study [18].

Fully optimizing the geometry of the S_1 state of the ring-based structure proved problematic, and so we froze the NMP moiety at the TD-CAM-B3LYP/aug-cc-pVTZ optimized geometry, and then optimized the position of the RG atom for the above-ring structure, again using the TD-CAM-B3LYP method. For NMP–Kr, we then relaxed and fully-optimized the structure, and found a minimum with an intermolecular bond length only 0.02 Å longer; although this procedure was still unsuccessful for NMP–Ar, the NMP–Kr result suggests that the unfreezing of the NMP moiety would make little difference to the calculated intermolecular separation.

4. Results

In Figs. 1 and 2 we present the REMPI spectra of NMP–Ar and NMP–Kr, respectively. In the case of NMP–Ar, these were recorded for the dominant isotopologue involving ^{40}Ar. In the case of NMP–Kr, the combined signals involving all naturally-occurring isotopes of Kr were recorded, since it is not anticipated that any isotopic differences will be discernible with the resolution of our lasers. As noted above, both one-colour and two-colour REMPI spectra were recorded, and these were found to be very similar. The spectra shown in Figs. 1 and 2 have been selected based on their quality and minimal interference from NMP resonances.

Although we scanned > 750 cm^{-1} to lower wavenumber and > 750 cm^{-1} to higher wavenumber, in both cases, signal was only obtained over a narrow range of wavenumbers (see Figs. 1 and 2); in particular, no structure was observed that is associated with excitation of the NMP-localized vibrational modes that were active in NMP itself. [2,16] Although chromophore-localized structure can be seen in the REMPI spectra of complexes of other molecules, such as complexes of phenol with methanol [21] and others,[22,23] often the focus is on the intermolecular bands associated with the origin transition, such as in work on complexes of substituted benzenes.[24,25] Interestingly, for complexes of benzene with rare gases, the symmetry lowers from $D_{6h} \rightarrow C_{6v}$ upon complexation, but the origin transition remains forbidden and so intermolecular modes have been studied in combination with the degenerate ν_6 vibration [26-28], which induces the vibronic activity in $S_1 \leftarrow S_0$ absorption spectrum. In the present case of NMP–RG complexes, the symmetry lowering causes the $S_1 \leftarrow S_0$ origin transition that is forbidden in NMP, to become allowed.

In line with the present quantum chemical calculations and microwave studies of the NMP–Ar complex [18], we assume that we observe the global minimum, with the RG atom above the ring. (Although it is possible that more than one isomer could be produced during the non-equilibrium conditions of the supersonic jet expansion, there is nothing in the REMPI or ZEKE spectra to suggest that there is more than one isomer present in the free-jet expansion.).

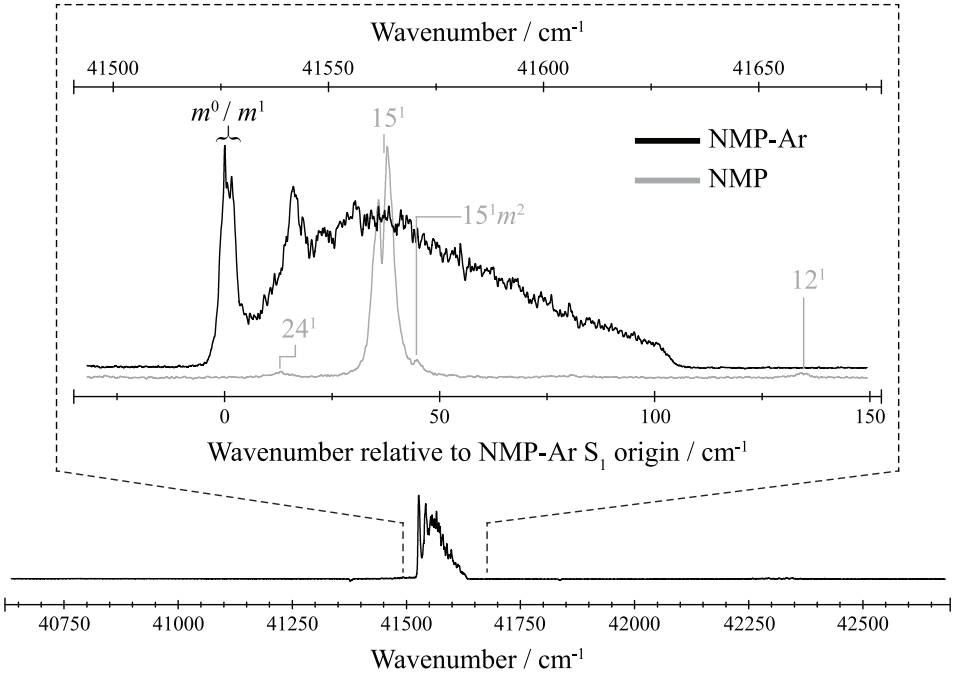

Fig. 1. (1 + 1′) REMPI spectrum of NMP–Ar (with the ionization laser set at 22916 cm^{-1}). The lower trace shows the spectrum over the full range scanned (1 cm^{-1} step size), showing that signals over a very limited wavenumber range were obtained. The upper trace shows a 0.2 cm^{-1} step-size scan of the NMP–Ar spectrum and, in grey, a section of the NMP spectrum, to indicate where accidental excitations of the monomer might occur. Although this is a cold spectrum, it is possible that signals from hot NMP complexes could contribute to the regions around these bands – these would be expected to be significantly weaker than the cold monomer bands, but still potentially significant compared to the much weaker complex signals.

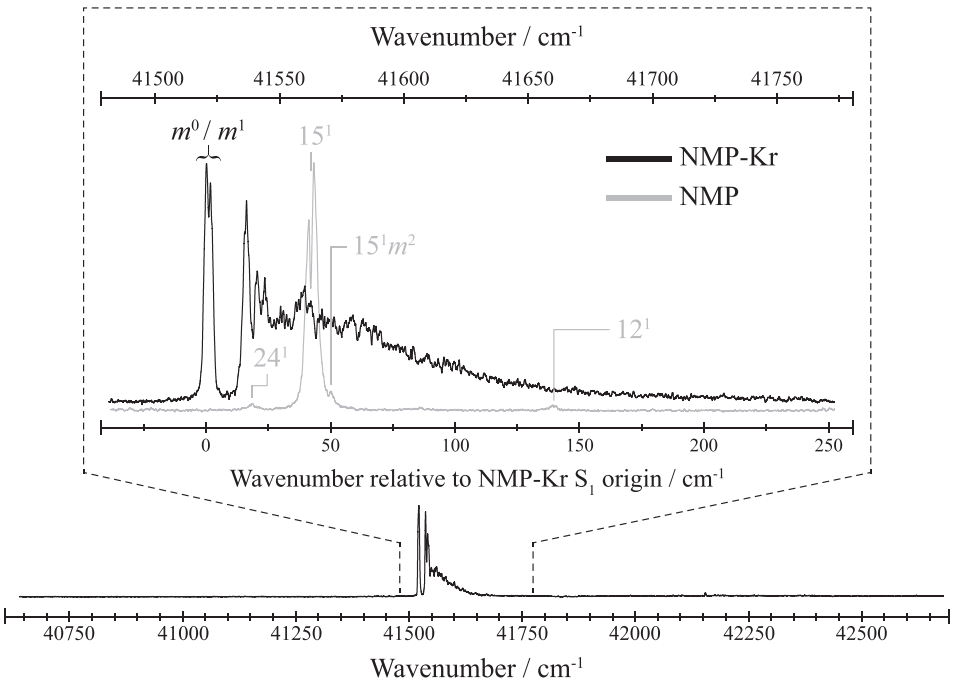

Fig. 2. (1 + 1) REMPI spectrum of NMP–Kr. The lower trace shows the spectrum over the full range scanned (1 cm^{-1} step size), showing that signals over a very limited wavenumber range were obtained (the weak feature at ca. 42240 cm^{-1} is spurious). The upper trace shows a 0.2 cm^{-1} step-size scan of the NMP–Kr spectrum and, in grey, a section of the NMP spectrum, to indicate where accidental excitations of the monomer might occur. Although this is a cold spectrum, it is possible that signals from hot NMP complexes could contribute to the regions around these bands – these would be expected to be significantly weaker than the cold monomer bands, but still potentially significant compared to the much weaker complex signals.

5. Assignments and discussion

5.1. REMPI spectra

The REMPI spectrum of NMP–Ar in Fig. 1 shows a strong band at 41527 cm^{-1}, which we shall conclude is the origin band, based upon the ZEKE spectra discussed in the next subsection; there is then a small gap followed by another discrete band, before a broad feature. To higher wavenumber is a well-defined drop in intensity marking the end of the observed spectrum. As mentioned above, and as shown in Fig. 1, we scanned a wide range of wavenumbers above and below this REMPI spectrum, and no other features were seen. We can immediately make several observations. First, that the appearance of the origin band in the one-photon electronic spectrum suggests that the presence of the Ar atom is sufficient to perturb the NMP electronic structure from its effective C_{2v} symmetry, such that the $\widetilde{A}^1A_2 \leftarrow \widetilde{X}^1A_1$ transition, dipole forbidden in NMP itself, becomes allowed. Secondly, the observation of the drop in intensity at higher wavenumber gives an estimate of the dissociation energy of the $\widetilde{A}$ state of NMP–Ar, D_0', of $\approx 105 \pm 2\,cm^{-1}$. Thirdly, the lack of observation of any other bands to higher or lower wavenumber suggests that the REMPI spectrum in Fig. 1 is associated with vibrationless NMP, and that levels associated with vibrational excitation of NMP in its $\widetilde{A}$ state are rapidly depopulated by some mechanism – presumably the presence of the low-frequency, anharmonic intermolecular vibrations accelerates the various processes that have been discussed for the short lifetimes of the NMP excited vibrational levels [2,10,11,12,13,14,15,16]. Fourthly, the spectrum is blue-shifted with respect to the NMP spectrum, whose origin is at 41193 cm^{-1} (Ref. [16]), indicating that the S_1 state of NMP–Ar is less-strongly bound than the S_0 state – see below.

Similar comments apply to the similar-looking REMPI spectrum of NMP–Kr shown in Fig. 2. Again, a strong origin band is seen at 41522 cm^{-1}, with some further structured bands, followed by a broad feature to higher wavenumber. This time there is no clear drop-off in intensity to higher wavenumber, but a gradual decay. Since diminishing Franck-Condon factors, for example, can also cause a loss of intensity in the spectrum, only lower-bound estimate of the dissociation energy of the $\widetilde{A}$ state, $D_0' \geq 170\,cm^{-1}$ can be deduced from where the NMP–Kr REMPI spectrum reaches the baseline at higher wavenumber. Again, the spectrum is blue-shifted with respect to that of NMP itself.

The spectra are very different to those observed previously for complexes of RG atoms with substituted benzenes, where discrete bands are seen with no significant unstructured region – in the case of toluene–RG complexes, which also have a hindered methyl rotor, the bands have been assigned to transitions involving intermolecular vibrations and hindered rotor levels [24,25]. In particular, we note that Gascooke and Lawrance [25] were able to identify contributions from a_1 and e symmetry levels, using 2D-LIF spectroscopy. We will make further comments regarding the REMPI spectra of the NMP–RG complexes, in the light of the ZEKE spectra, in the next subsection.

Regarding the nature of the electronic structure, it is known that the S_1 state of NMP, arising from a 3s ← π excitation, is Rydberg-like in the Franck-Condon region. For the S_1 state of the NMG–RG complexes, we have both a 3s Rydberg electron and the RG atom each competing for the NMP^+ cationic core. This situation is reminiscent of the $\widetilde{A}\,^2\Sigma^+$ states of the NO–RG complexes, corresponding to a 3s ← π* excitation on NO, where the state was unbound for RG = Ne [29], and weakly bound for RG = Ar, Kr and Xe [30-32], with the interaction becoming stronger as the polarizability of RG increased, but all significantly more weakly-bound than the corresponding cations. As here, the REMPI spectrum of NO–Ar was blue-shifted with respect to the corresponding transition in NO, indicating the $\widetilde{A}$ state was less strongly bound than the $\widetilde{X}$ state. This was explained in terms of the competition between the low-lying 3s Rydberg electron and the RG atom for the NO^+ cationic core. For the S_1 states of the NMP–RG complexes, we also conclude that the interaction of the RG atom with the NMP^+ core is weakened by the presence of the low-lying 3s electron, so that the RG atom largely is interacting with a neutral molecule, rather than wholly with the cationic core. This is in-line with the calculated S_1 optimized geometry, notably the significantly longer intermolecular bond lengths than in the S_0 state.

5.2. ZEKE spectra

We show the low-wavenumber regions of ZEKE spectra recorded for NMP–Ar and NMP–Kr in Figs. 3 and 4, respectively.

When exciting via the origin band, well-defined structure can be seen in the ZEKE spectra at low wavenumber; the structure is somewhat

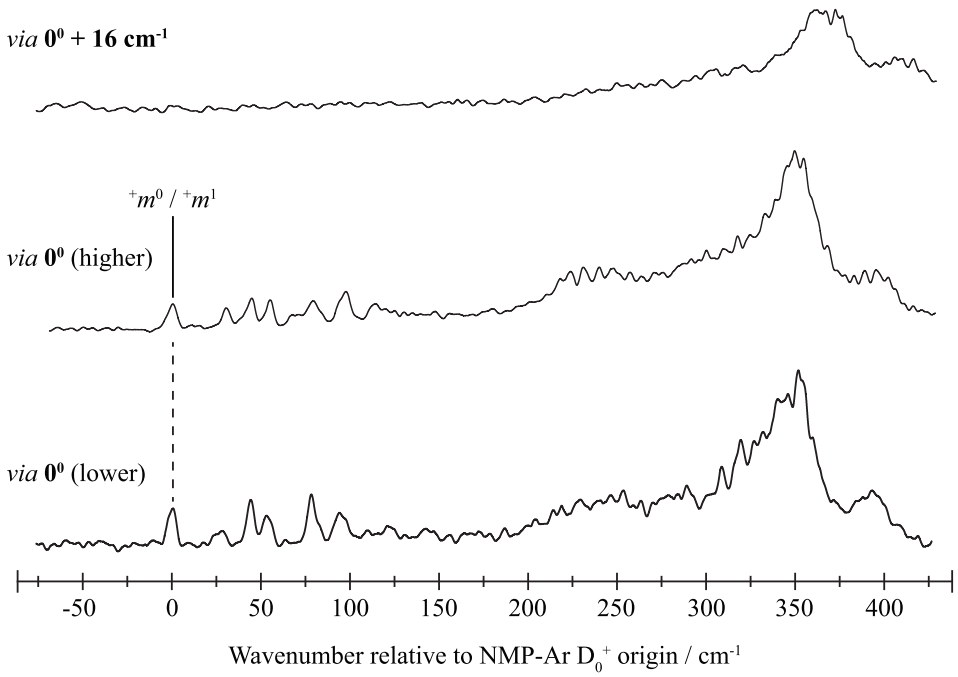

Fig. 3. Low-wavenumber region of ZEKE spectra of NMP–Ar exciting through the indicated levels. Assignments have only been given for the lowest wavenumber band, since many of the levels are expected to have mixed character owing to Fermi resonances and vibration-torsional coupling – see text.

clearer for NMP–Kr than it is for NMP–Ar. This structure is likely to arise from a mixture of torsional and intermolecular vibrations in the D_0^+ state, as seen for the S_0 and S_1 states of toluene–RG (RG = Ar–Xe) by Mons et al. [24] and toluene–Ar by Gascooke and Lawrance [25]. In our previous work on NMP [1], it was found that a $\Delta m = 0$ propensity rule was strongly adhered to – this was in line with the Rydberg-like nature of the S_1 state of NMP in the Franck-Condon region. The NMP–RG complexes differ from NMP in several ways: the symmetry is lowered, making the electronic transition allowed; the torsional potential for NMP–RG will not be the same as for NMP itself, with the introduction of a V_3 term into the torsional potential if the RG atom lies along the z axis of the complex, with other V_n terms arising if the RG atom is positioned asymmetrically; the S_1 state is not expected to be Rydberg-like (see below).

We first address the fact that we might expect to see two different origins, corresponding to the m^0 and m^1 transitions in the REMPI spectrum. The splitting between the first two main REMPI bands is too large to be these, as seen, for example, by comparing to the distinct origins seen for *m*-fluorotoluene [33-35] and *o*-fluorotoluene [33]. The first REMPI bands here do show a small splitting, but the ZEKE spectra from each are essentially identical (see Figs. 3 and 4), and so we associate this with overlapping, unresolved rotational structure. As a consequence, we conclude that the m^0 and m^1 transitions are heavily overlapped in our spectra (we note that these are separated by only 0.9 cm^{-1} in toluene–Ar [25]). For *m*-fluorotoluene, which also has G_6 molecular symmetry, significant torsional structure is seen in the ZEKE spectrum; in addition, there is a change in the sign of the potential upon ionization leading to the $\Delta m = 0$ propensity rule not being followed [35,36]. For NMP, the phase of the potential does not change between the S_1 and D_0^+ states [1], and so we do expect the $\Delta m = 0$ propensity rule to be followed; hence, we would expect to see a strong, overlapped $^+m^{0,1}$ ZEKE band, with less-intense, but sizeable $^+m^2$, $^+m^{3(+)}$ and $^+m^4$ ($\Delta m = 3$) bands; contributions from the $\Delta m = 6$ bands and others would be expected to be weak.

We expect the torsional levels will also be similar to those of NMP^+ reported in Ref.1. We refrain from giving specific assignments except for the origin bands, since: some bands are overlapped; each band has a width arising from unresolved rotational structure and some are asymmetric; some intermolecular levels are likely to be in Fermi resonance [24,25]; and there is likely to be coupling between torsional and intermolecular vibrational levels forming "vibtor" eigenstates [25] – thus, levels may have varying admixtures of intermolecular and torsional character. Given the preceding discussion, and the present resolution in the ZEKE spectra, we do not feel we can extract any further detailed information of the make-up of the cationic intermolecular vibration/torsion states in the NMP–RG complexes, nor can we determine the V_n and F parameters in the torsional potential. (Even in the microwave study of NMP–Ar [18], the V_6 parameter had to be assumed to be the same as that for NMP within the fit.)

Taking the first band in each ZEKE spectrum as the adiabatic ionization energy (AIE), gives values of 64077 ± 5 cm^{-1} for NMP–Ar, and 64029 ± 5 cm^{-1} for NMP–Kr. These suggest stabilization of the NMP cation by 173 cm^{-1} and 221 cm^{-1} for each of Ar and Kr, respectively. (Note that we do not correct the AIE for the applied field, since such corrections are imprecise, particularly for larger molecules where decay of the lower-lying Rydberg states means the true field-shifted ionization energy onset is seldom seen [37]).

When we excited via the level associated with the second discrete band in the REMPI spectrum for NMP–Ar at $0^0 + 16$ cm^{-1}, we find that the low-wavenumber structure is absent (Fig. 3), with only broad structure to higher wavenumber. We suggest that, comparing with the observations in NMP–Kr, this indicates that the transition intensity to the intermolecular modes has been dissipated to numerous cation levels, but since the transitions are weaker than those in NMP–Kr, each is too weak to be discerned in the present work. In the NMP–Kr spectrum (Fig. 4), however, significant structure can be seen when exciting through other levels, although the intensities of the different bands vary significantly. For example, when exciting the second band ($0^0 + 16$ cm^{-1}), it can be seen that the origin is much less intense, but that there is a plethora of activity up to ~300 cm^{-1}. This is consistent with a significant change in the intermolecular potential upon ionization. It is possible that the second REMPI band consists of overlapped intermolecular bend and m^2 torsional transitions, for both complexes. We cannot be certain of the assignment of the other two bands in the NMP–Kr REMPI spectrum; but since they are too low in wavenumber to be overtones or other torsional levels, we suggest that one arises from the second bending mode, while the other is the stretch, but the ordering

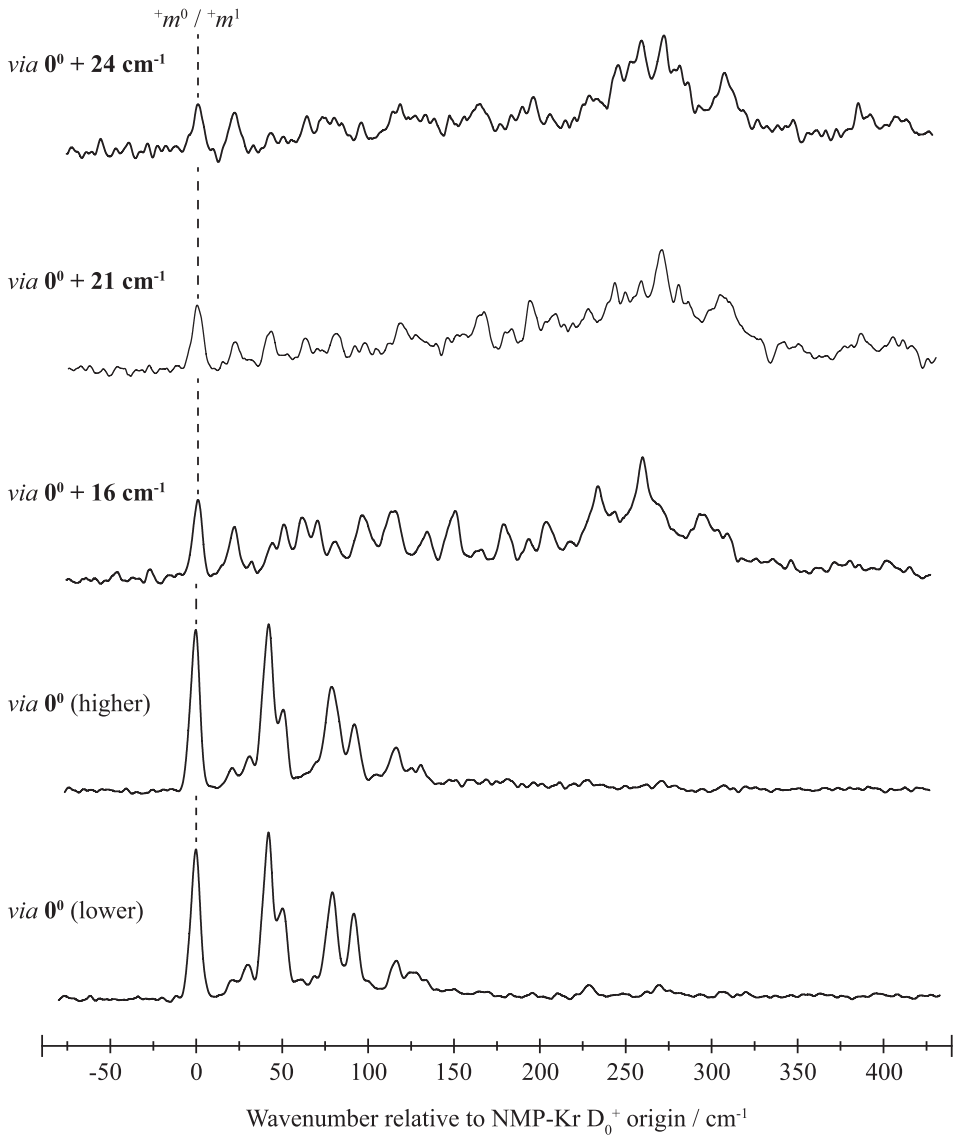

Fig. 4. Low-wavenumber region of ZEKE spectra of NMP–Kr exciting through the indicated levels. Assignments have only been given for the lowest wavenumber band, since many of the levels are expected to have mixed character owing to Fermi resonances and vibration-torsional coupling – see text.

is not obvious.

It is difficult to ascribe the unstructured region of the REMPI spectrum wholly to significant coupling between S_1 state intermolecular and torsional levels, and so it may arise from rapid internal conversion, intersystem crossing or from coupling to levels around the barrier to dissociation, i.e. mechanisms discussed in other studies on NMP [2,12,14,16], but all enhanced by both the presence and the anharmonicity of the intermolecular motions. This is notable, since this lack of structure is present at very low internal energies; indeed, even low-energy torsional levels, such as $m^{3(+)}$ and m^4, both observed in uncomplexed NMP [1], are seemingly contained within this broad feature. In other ZEKE spectra (not shown), other bands, often broad, were seen to higher energy than the features shown in Figs. 3 and 4, and this was particularly the case when exciting within the broad features of the REMPI spectra. Several of these appear to be associated with excitation of the NMP monomer – for example, coincidentally exciting the 24^1 band or 15^1 bands (see Figs. 1 and 2). It is not possible that the NMP–RG complexes have dissociated to form NMP + RG at these low energies. In addition, to still higher wavenumber than that shown, effects were seen in all ZEKE spectra arising from the presence of Wood's and Rayleigh anomalies associated with the 2400 l/mm grating employed in the ionization dye laser, as discussed in Ref. 3, to which the reader is referred for further commentary; as such, we do not discuss this further here. In the future, recording higher wavenumber regions of the ZEKE spectra with a different grating and/or mass-analyzed threshold ionization (MATI) spectra, would likely give further insight into whether any NMP-localized vibrational excitation is present in the photoionization spectra of these complexes.

5.3. Binding energies

In the above for NMP–Ar, we have deduced a value of $D_0 \approx 105\ \mathrm{cm}^{-1}$ for the S_1 state, and using the T_0' values for NMP and NMP–Ar, we obtain a value for the S_0 state, $D_0'' = 440\ \mathrm{cm}^{-1}$. Similarly, for NMP–Kr, a lower bound value of $D_0 \geq 170\ \mathrm{cm}^{-1}$ is found for the S_1 state, and using the T_0' values for NMP and NMP–Kr, we obtain a lower-bound value for D_0'' of $\geq 500\ \mathrm{cm}^{-1}$. It can be seen that both of these values are consistent with the calculated CCSD(T) values in Table 1. In contrast, it can be seen that the CAM-B3LYP binding energies are significantly different to the CCSD(T) ones, and in poor agreement with experiment.

When each AIE is combined with the $D_0^+ \leftarrow S_1$ ionization energy of the relevant complex, and using the AIE of NMP from Ref. 1, then using

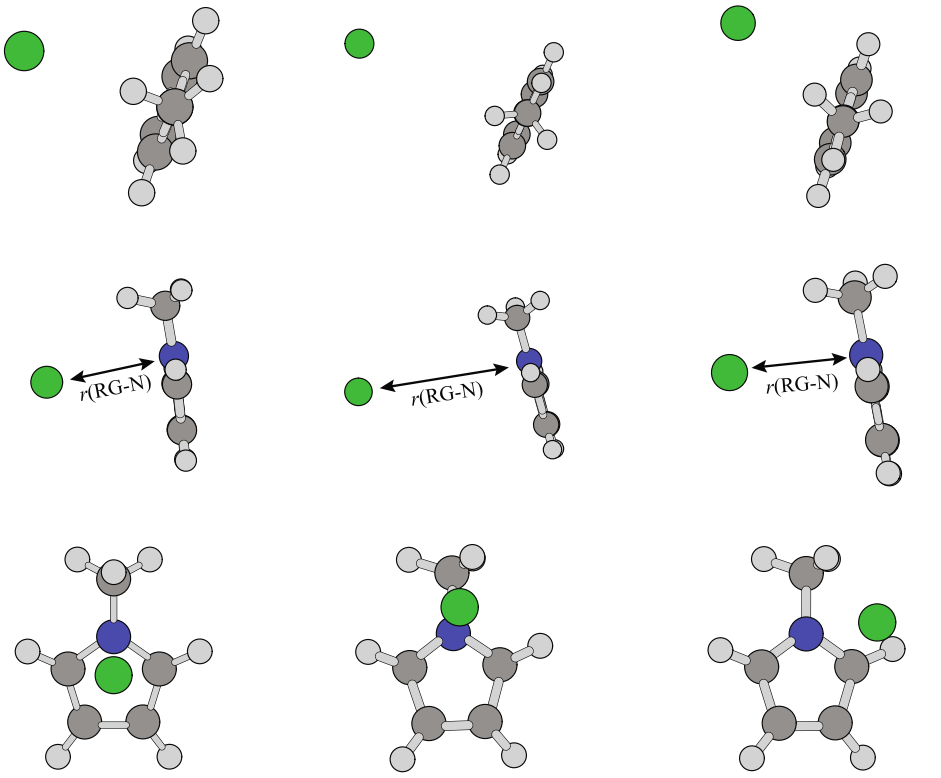

Fig. 5. Calculated geometries of NMP–RG using the indicated levels of theory. Owing to difficulties with the full optimization, for the S_1 state of NMP–Ar, the NMP ring was fixed at its TD-CAM-B3LYP/aug-cc-pVTZ-optimized geometry, and the position of the Ar atom was optimized; for NMP–Kr, a full optimization was successful [with a similarly constrained optimization giving a *r*(Kr–N) distance only 0.02 Å longer]. Cartesian coordinates for the optimized structures are given in the Supplementary Material.

Table 1
Calculated and experimental binding energies (cm^{-1}) for NMP–Ar and NMP–Kr.

NMP–RG		CAM–B3LYP[a,b]	(R)CCSD(T)[a]			Expt[d]
			BSSE (RG)	BSSE (NMP)	RCCSD (T)[c]	
NMP–Ar	S_0	87	108	31	429	440
	S_1					105
	D_0^+	262	106	27	534	610
NMP–Kr	S_0	85	81	33	517	≥ 500
	S_1					≥ 170
	D_0^+	343	86	28	690	≥ 720

[a] D_e value, i.e. no correction for zero-point energies.
[b] Not counterpoise corrected.
[c] Counterpoise corrected.
[d] Approximate D_0 values – see text. The values for NMP–Kr are based on the high-wavenumber offset in the REMPI spectrum, which is taken as a lower bound for D_0 in the S_1 state; thus, the values for the S_0 and D_0^+ states are also lower bounds. For NMP–Ar, there is a better-defined offset, and so the uncertainty in the S_1 binding energy value is likely ca. $\pm 2\ cm^{-1}$, and this uncertainty will contribute to the values for the other states also. For the S_0 state, the uncertainty will be similar, while with regard to the cation, for NMP^+–Ar, the broader ZEKE bands mean that the uncertainty is likely $\pm 5\ cm^{-1}$.

the S_1 dissociation energies above, one obtains values for the dissociation energy of the cation complexes as $D_0 \approx 610\ cm^{-1}$ for NMP^+–Ar, and $D_0 \geq 720\ cm^{-1}$ for NMP–Kr. Again, it can be seen that the value for NMP–Kr is close to the calculated RCCSD(T) values in Table 1, while the agreement with the calculated value for NMP–Ar is reasonable, but not as good.

This poor performance of the CAM-B3LYP method with regard to the binding energies, observing that these would be even lower if these were corrected for basis set superposition error, leads us to conclude that the calculated intermolecular wavenumbers should only be used in a qualitative manner, particularly given their low harmonic values, and the expected anharmonicities of the actual vibrations; as such, we do not report these explicitly. Of course, this also suggests that caution is required in employing the CAM-B3LYP geometries in the RCCSD(T) calculations for the binding energies. We note that the calculated intermolecular bond length here of $R_e = 3.67$ Å is not too far from the microwave *R* value of 3.448 Å for the S_0 state, and so we feel the CAM–B3LYP structures are likely to be fair indications of the actual structures, which is supported by the reasonable agreement of the (R)CCSD(T) binding energies with experiment.

Overall, it is clear that basis set superposition error (BSSE) is playing a significant role here (see Table 1), and so larger basis sets might be expected to be advantageous, as would using geometries optimized at higher levels of theory; however, each of these is computationally expensive.

6. Conclusions

We have reported REMPI spectra for NMP–Ar and NMP–Kr. We believe we have seen the origin transition, implying that the perturbation of the NMP electronic structure is sufficient to render this a dipole-allowed transition. Further, both spectra are blue-shifted with respect to the NMP origin, consistent with the S_1 states being more weakly bound than the S_0 state. In addition, the activity in the REMPI spectra was localized to the region around the origin, with no activity seen for

excited NMP-localized vibrations, interpreted in terms of the low-frequency intermolecular modes exacerbating coupling between levels, shortening their lifetimes. It would be interesting to record REMPI spectra of these species using picosecond lasers, to ascertain whether the absence of NMP-localized excited vibrational bands in the present work is due to their short lifetime. It would also be of interest to investigate other ligands.

We have discussed the origin of the low-wavenumber structure in the ZEKE spectra in terms of torsional and intermolecular transitions during the ionization, and we were able to obtain AIEs for both complexes, but not detailed information on the torsional potentials. Possibly 2D-LIF spectra over the electronic absorption spectrum might also prove useful in identifying torsional and intermolecular bands, as it was in the case of toluene–Ar [25]; however, this relies on being able to distinguish between bands of a_1 and e symmetry, and hence on the separation of the m^0 and m^1 bands in the excitation spectrum, which may well not be possible in the present case.

From the REMPI and ZEKE spectra, we were able to deduce estimates of binding energies, and these generally agreed well with calculated values at the (R)CCSD(T) level for the S_0 and D_0^+ states, although those at the CAM-B3LYP level were not in good agreement. MATI spectra would be a means of confirming the deduced binding energies in the cation. Indeed, such binding energies have been measured [38] with the MATI technique to yield values of *p*-fluorotoluene–Ar in the S_0 and D_0^+ states as 329 cm^{-1} and 510 cm^{-1}, respectively; these compare well to the present respective values for NMP–Ar of 440 cm^{-1} and 610 cm^{-1}.

CRediT authorship contribution statement

Alexander R. Davies: Investigation, Writing – review & editing, Visualization, Data curation. **Jessica T.L. Haynes:** Investigation, Data curation. **Timothy G. Wright:** Conceptualization, Writing – original draft, Investigation, Validation, Supervision, Project administration, Funding acquisition.

Declaration of Competing Interest

The authors declare that they have no known competing financial interests or personal relationships that could have appeared to influence the work reported in this paper.

Data Availability Statement

The data that support the findings of this study are available from the corresponding author upon reasonable request.

Acknowledgements

We thank the University of Nottingham for a studentship to A.R.D. We are grateful for access to the University of Nottingham High Performance Computing Facility.

References

[1] A.R. Davies, D.J. Kemp, T.G. Wright, Chem. Phys. Lett. 763 (2021), 138227.
[2] A.R. Davies, D.J. Kemp, T.G. Wright, J. Chem. Phys. 154 (2021), 224305.
[3] A.R. Davies, D.J. Kemp, T.G. Wright, J. Chem. Phys. 155 (2021), 117101.
[4] A.R. Davies, D.J. Kemp, T.G. Wright, J. Molec. Spec. 376 (2021), 111410.
[5] G. Milazzo, Gazz. Chim. Ital. 74 (1944) 152.
[6] R. McDiarmid, X. Xing, J. Chem. Phys. 105 (1996) 867.
[7] J.G. Philis, Chem. Phys. Lett. 353 (2002) 84.
[8] J.G. Philis, J. Molec. Struct. 651–653 (2003) 567.
[9] N. Biswas, S. Wategaonkar, J.G. Philis, Chem. Phys. 293 (2003) 99.
[10] A.G. Sage, M.G.D. Nix, M.N.R. Ashfold, Chem. Phys. 347 (2008) 300.
[11] C.-M. Tseng, Y.T. Lee, C.-K. Ni, J. Phys. Chem A 113 (2009) 3881.
[12] L. Blancafort, V. Ovejas, R. Montero, M. Fernández-Fernández, A. Longarte, J. Phys. Chem. Lett. 7 (2016) 1231.
[13] G. Piani, L. Rubio-Lago, M.A. Collier, T. Kitsopoulos, M. Becucci, J. Phys. Chem. A 113 (2009) 14554.
[14] G. Wu, S.P. Neville, O. Schalk, T. Sekikawa, M.N.R. Ashfold, G.A. Worth, A. Stolow, J. Chem. Phys. 144 (2016), 014309.
[15] T. Geng, O. Schalk, T. Hansson, R.D. Thomas, J. Chem. Phys. 146 (2017), 144307.
[16] K.C. Woo, S.K. Kim, Phys. Chem. Chem. Phys. 21 (2019) 14387.
[17] J.R. Gascooke, W.D. Lawrance, J. Phys. Chem. A 126 (2022) 2160.
[18] S. Huber, J. Makarewicz, A. Bauder, Molec. Phys. 95 (1998) 1021.
[19] V.L. Ayles, C.J. Hammond, D.E. Bergeron, O.J. Richards, T.G. Wright, J. Chem. Phys. 126 (2007), 244304.
[20] T. Yanai, D.P. Tew, N.C. Handy, Chem. Phys. Lett. 393 (2004) 51.
[21] T.G. Wright, E. Cordes, O. Dopfer, K. Müller-Dethlefs, J. Chem. Soc. Faraday Trans. 89 (1993) 1609.
[22] O. Dopfer, T.G. Wright, E. Cordes, K. Müller-Dethlefs, J. Electron Spectrosc. Rel. Phenom. 68 (1994) 247.
[23] K. Müller-Dethlefs, O. Dopfer, T.G. Wright, Chem. Rev. 94 (1845) 1994.
[24] M. Mons, J. Le Calvé, F. Piuzzi, I. Dimicoli, J. Chem. Phys. 92 (1990) 2155.
[25] J.R. Gascooke, W.D. Lawrance, J. Chem. Phys. 138 (2013), 084304.
[26] M. Schmidt, M. Mons, J. Le Calvé, Chem. Phys. Lett. 177 (1991) 371.
[27] T. Weber, E. Riedle, H.J. Neusser, E.W. Schlag, Chem. Phys Lett. 183 (1991) 77.
[28] H. Shinohara, S. Sato, K. Yoshihara, K. Kimura, J. Electron Spectrosc. Rel. Phenom. 88 (1998) 131.
[29] V.L. Ayles, R.J. Plowright, M.J. Watkins, T.G. Wright, J. Kłos, M.H. Alexander, P. Pajón-Suarez, J. Rubayo-Soneira, R. Hernández-Lamoneda, Chem. Phys. Lett. 441 (2007) 181.
[30] S.D. Gamblin, S.E. Daire, J. Lozeille, T.G. Wright, Chem. Phys. Lett. 325 (2000) 232.
[31] J. Lozeille, S.E. Daire, S.D. Gamblin, T.G. Wright, D.M. Smith, J. Chem. Phys. 113 (2000) 7224.
[32] J. Kłos, M.H. Alexander, R. Hernández-Lamoneda, T.G. Wright, J. Chem. Phys. 129 (2008), 244303.
[33] K. Okuyama, N. Mikami, M. Ito, J. Phys. Chem. 89 (1985) 5617.
[34] L.D. Stewart, J.R. Gascooke, W.D. Lawrance, J. Chem. Phys. 150 (2019), 174303.
[35] D.J. Kemp, E.F. Fryer, A.R. Davies, T.G. Wright, J. Chem. Phys. 151 (2019), 084311.
[36] K. Takazawa, M. Fujii, M. Ito, J. Chem. Phys. 99 (1993) 3205.
[37] X. Zhang, J.M. Smith, J.L. Knee, J. Chem. Phys. 97 (1992) 2843.
[38] S. Georgiev, T. Chakraborty, H.J. Neusser, J. Phys. Chem. A 108 (2004) 3304.